Coherent generation of phonon-polaritons in $Bi_2Sr_2CaCu_2O_{8+x}$ intrinsic Josephson junctions

Sven-Olof Katterwe, Holger Motzkau, Andreas Rydh, and Vladimir M. Krasnov[*]

Department of Physics, Stockholm University, AlbaNova University Center, SE-10691 Stockholm, Sweden
(Received 13 January 2011; published 17 March 2011)

The $Bi_2Sr_2CaCu_2O_{8+x}$ high-temperature superconductor represents a natural layered metamaterial composed of metallic CuO bilayers sandwiched between ionic BiO planes. Each pair of CuO bilayers forms an atomic-scale Josephson junction. Here we employ the intrinsic Josephson effect for *in situ* generation and self-detection of electromagnetic waves in $Bi_2Sr_2CaCu_2O_{8+x}$ single crystals. We observe that electromagnetic waves form polaritons with several transverse optical phonons. This indicates the presence of unscreened polar response in cuprates, which may lead to unusually strong electron-phonon interaction. Our technique can provide intense local sources of coherent, monochromatic phonon-polaritons with kW/cm^2 power densities.

Propagation of light in a media is accompanied by electromagnetic (EM) interaction with charged particles. The interaction is strong in polar materials such as ionic insulators and ferroelectrics. Resonances between light and EM-active collective modes in the media (e.g., optical phonons or excitons[1,2]) lead to formation of polaritons, half light–half matter particles, with a singular dielectric function

$$\epsilon_r(\omega) = \epsilon_\infty + \sum_j \frac{\omega_{TO,j}^2 S_j}{\omega_{TO,j}^2 - \omega^2 - i\gamma_j\omega}. \qquad (1)$$

It has poles at transverse ω_{TO} and zeros at longitudinal ω_{LO} optical frequencies. Here S_j and γ_j are oscillator strengths and damping parameters, respectively. Light does not propagate through the media at $\omega_{TO} < \omega < \omega_{LO}$ for the same reason that low-frequency EM waves do not propagate through metals, namely, due to the negative dielectric constant $Re(\epsilon_r) < 0$. For $\gamma \to 0$, the group velocity of light turns to zero at ω_{TO}. The ability of polaritons to slow down, or even stop and store photons,[3] has attracted significant attention in recent years because it may be used in optical metamaterials and facilitate manipulation of photons in polaritonics.[4]

Here we study EM-wave propagation in the layered high-temperature superconductor $Bi_2Sr_2CaCu_2O_{8+x}$ (Bi-2212). Superconductivity in cuprates occurs as a result of doping of the parent ionic oxide insulator. Optical spectroscopy has revealed an intermixture of metallic (Drude-type anomaly at $\omega = 0$) and ionic [strong infrared (IR) phonons] properties in cuprates.[5–7] However, Bi-2212 is not a uniform doped Mott insulator. It represents a natural atomic superlattice composed of metallic CuO_2-Ca-CuO_2 bilayers sandwiched between ionic SrO-2BiO-SrO planes. Most clearly, this was demonstrated by observation of the intrinsic Josephson effect between CuO bilayers.[8–10] From an optical point of view, Bi-2212 represents a layered metamaterial,[3,11,12] i.e., a multilayer transmission line for EM waves. Therefore, low-frequency transverse EM (TEM) waves can propagate along insulating BiO planes[13] despite the fact that Bi-2212 is metallic. Importantly, the intrinsic Josephson effect allows both *in situ* generation and detection of TEM waves in the crystal, i.e., the material as such can convert the dc bias current into high-frequency ac electric field via the quantum mechanical ac Josephson effect.

We study small mesa structures, fabricated on top of Bi-2212 single crystals using microfabrication and nanofabrica-

tion techniques. We use two batches of crystals: pure, slightly underdoped Bi-2212 with critical temperature $T_c \simeq 82$ K, and lead-doped, slightly overdoped $Bi_{2-y}Pb_ySr_2CaCu_2O_{8+x}$ with $T_c \simeq 87$–91 K. The most noticeable difference between them is in the c-axis critical current density $J_c(4.2 \text{ K}) \simeq 10^3$ and 10^4 A/cm^2 for pure and lead-doped mesas, respectively. Measurements were performed in a gas-flow ^{4}He cryostat in a temperature range down to 1.6 K and magnetic field H up to 17 T. Samples were mounted on a rotatable sample holder. Accurate alignment of the field parallel to CuO planes was needed to avoid intrusion of Abrikosov vortices in intense magnetic fields. For alignment, we used the procedure developed in Ref. 10, which facilitates alignment with an accuracy better than $0.02°$. Details of sample fabrication and measurements can be found in Refs. 10 and 13.

The inset of Fig. 1 shows current-voltage (I-V) characteristics of a lead-doped mesa (M1, 1.3×1.9 μm^2). Periodic branches are due to one-by-one switching of junctions from the superconducting to the quasiparticle (QP) state.[8,14] Additional small sub-branches are seen at every QP branch. They represent resonances between the ac Josephson oscillations in intrinsic junctions and c-axis LO phonons.[15–18] Figure 1 shows temperature dependence of the first QP branch for the same mesa. Unlike the superconducting gap and QP resistance, which decrease with increasing T,[14] the voltages of phonon resonances remain independent of T and correspond to frequencies of IR and Raman active c-axis phonons.[5,6,19] In total, 14 LO phonons could be recognized (marked by dashed lines in Figs. 1 and 4). The eight strongest are identified in Table I.

The amplitude of phonon resonances is proportional to J_c^2.[18] Since J_c for our lead-doped crystals is about 10 times larger than for pure Bi-2212 crystals, phonon resonances in the lead-doped mesas are greatly enhanced. Observation of resonances in pure Bi-2212 requires analysis of dI/dV characteristics.[17] Similarly, resonances are strongly suppressed by a moderate c-axis magnetic field due to penetration of Abrikosov vortices, which suppress superconductivity[20] and J_c. In contrast, in-plane magnetic field up to 17 T is not affecting superconductivity and J_c at $T \ll T_c$ due to the extremely large anisotropy of Bi-2212. The apparent Fraunhofer modulation of the c-axis critical current in this case[10] is caused by interference of opposite supercurrents, circulating in Josephson fluxons, with unsuppressed amplitude J_c.
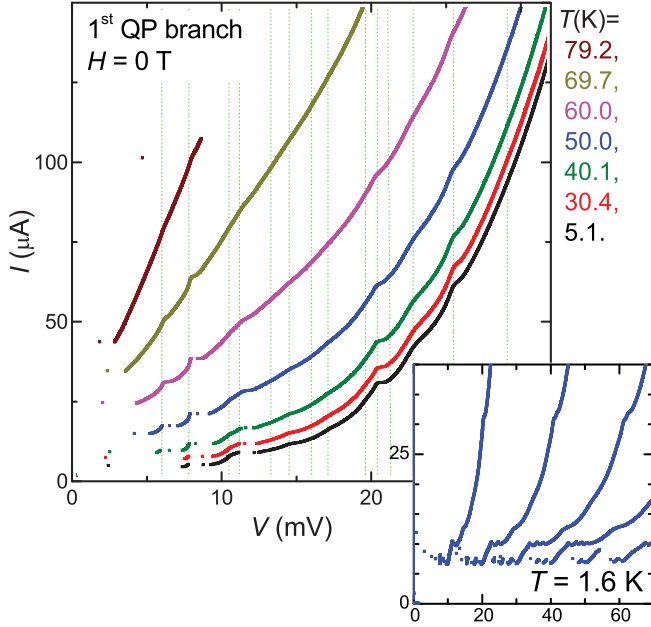
FIG. 1. (Color online) Temperature dependence of the first QP branch for the lead-doped mesa M1 in zero magnetic field. It is seen that phonon frequencies are T independent. The inset shows QP branches in the I-V of the same mesa at $T = 1.6$ K. Resonances with LO phonons are seen at every QP branch.

At sufficiently large magnetic field, fluxons form a regular lattice in the mesa.[10] The number of fluxons per junction is given by the ratio Φ/Φ_0, where $\Phi = HLs$ is the flux per junction, L is the junction length, $s \simeq 1.5$ nm is the stacking periodicity of intrinsic junctions, and Φ_0 is the flux quantum. The c-axis bias current exerts a Lorentz force and causes unidirectional fluxon motion. This leads to the appearance of an additional flux-flow branch in the I-V curve, with the voltage per junction $V_{\mathrm{FF}} = u_{\mathrm{FF}} Hs$, where u_{FF} is the flux-flow velocity. Periodic collision of fluxons with the edge of the mesa leads to flux-flow oscillations.[13,21] Produced EM waves are partly emitted and partly reflected back into the mesa. The latter start to travel as TEM waves in the multilayered transmission line formed by the mesa get reflected at the opposite edge, and continue bouncing until decay.

Figure 2 shows the flux-flow part of the I-V for a lead-doped mesa (M2, 1.2×2 μm^2) measured during continuous sweep of the in-plane magnetic field from 4.2 to 4.4 T. The

TABLE I. Identification of LO phonon resonances at zero field, marked in Fig. 1 (following Ref. 6).

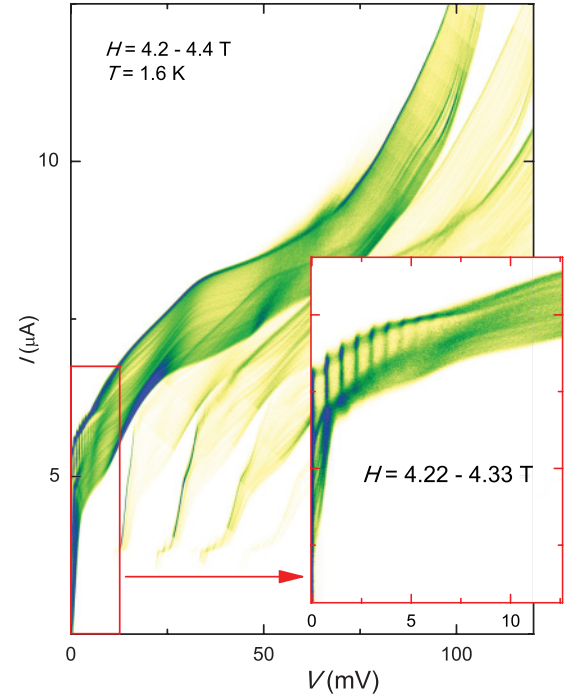| No.	V (mV)	ω_{LO} (cm^{-1})	Type	Symmetry	Assignment
1	6.0	97	IR	A_{2u}	Bi′:Cu1CaSr
2	7.8	126	Raman	A_{1g}	Cu1Sr
3	10.5	169	IR	A_{2u}	Sr:Cu1′
4	11.2	181	Raman	A_{1g}	Sr:Cu1′
5	14.5	234	IR	A_{2u}	Ca:Sr′
6	20.4	329	IR	A_{2u}	O3O1
7	22.8	368	IR	A_{2u}	O1′:CaO3
8	25.5	411	Raman	A_{1g}	O1:Sr′

FIG. 2. (Color online) Flux-flow part of the I-V for the lead-doped mesa M2, measured during continuous sweep of the in-plane magnetic field from 4.2 to 4.4 T. The inset shows a series of Fiske steps, caused by formation of standing waves inside the mesa. It demonstrates the Josephson flux-flow mechanism of TEM wave generation in our experiment.

flux-flow voltage grows gradually with H. Bouncing TEM waves can be explicitly visualized at geometrical resonance conditions, corresponding to formation of standing waves in the mesa. They are seen as a series of Fiske steps on the flux-flow branch.[13] We note that those TEM waves are photonlike because they have a linear dispersion relation at low frequencies. This leads to equidistance of Fiske steps. The inset in Fig. 2 demonstrates Fiske steps, corresponding to out-of-phase oscillations in neighboring junctions with one node per junction.[13] The deduced TEM wave speed $c_N \simeq 3.9 \times 10^5$ m/s is almost 1000 times slower than the speed of light in vacuum; this is not because of the extraordinary large ϵ_r, but it is due to an extraordinary large kinetic inductance of the atomically thin intrinsic junctions.

The strongest geometrical resonance occurs at the velocity-matching condition when u_{FF} is equal to the phase velocity of TEM waves.[13] In this case, waves are synchronized with the fluxon chain and the wavelength is equal to the separation between fluxons. The corresponding in-plane wave number is

$$k = 2\pi Hs/\Phi_0. \qquad (2)$$

It can be easily tuned by changing H. In experiment, the velocity-matching resonance is seen as a sharp upturn (maximum in dI/dV) at the top of the flux-flow branch. The corresponding frequency is given by the ac Josephson relation

$$\omega = 2\pi V_{\mathrm{FF}}^*/\Phi_0, \qquad (3)$$

where V_{FF}^* is the measured maximum flux-flow voltage per junction. Equations (2) and (3) provide the basis for analysis of the dispersion relation in this work.

Figure 3 shows I versus V per junction at different in-plane magnetic fields for a lead-doped mesa (M3, 0.9×1.3 μm^2) with $N = 11$ junctions. The velocity-matching flux-flow step is marked by circles. It is moving to higher voltages with increasing H and eventually saturates close to the voltage of phonon number 2 in Table I. Above it, we observe a series of additional, remarkably strong resonances. The first three are marked by squares, rhombuses, and triangles. Each series has $N = 11$ sub-branches with voltages $V_j = (N - j)V_{FF} + jV_R$ ($j = 1, 2, \ldots, N$) due to one-by-one switching of all junctions from the flux-flow V_{FF} to the resonance state V_R. The last sub-branch in each series represents the flux-flow and phonon resonance frequency. These new types of resonances develop gradually out of one of the LO phonon resonances at $H = 0$, *grow in amplitude*, and move to higher voltages with increasing field.

Figure 4 presents our main result: voltage per junction of flux-flow and phonon resonances versus H, which are translated into the dispersion relation ω versus k via Eqs. (2) and (3). Figure 4(a) shows the dispersion relation for the

mesa M3. The lowest dispersion branch represents the regular flux-flow branch, indicated by circles in Fig. 3. It is roughly linear at low k, corresponding to a constant speed of light $\simeq 4 \times 10^5$ m/s close to the out-of-phase TEM velocity, obtained independently from the analysis of Fiske steps.[13] At larger k ($H > 12$ T), we observe a clear saturation with the group velocity $d\omega/dk \to 0$ when the flux-flow frequency becomes close to the lowest Raman phonon number 2 in Table I. Higher dispersion branches correspond to phonon resonances, as indicated in Fig. 3. They start flatly from a certain LO phonon frequency at $k = 0$ (indicated by horizontal lines), grow at intermediate k, and saturate again upon approaching the next TO phonon.[22] Figure 4(b) demonstrates a similar behavior of mesa M1, which is slightly more overdoped and has about 30% larger J_c. Figure 4(c) shows data for a pure Bi-2212 mesa. Since phonon resonances are much weaker here due to smaller J_c, we are able to trace interaction only with the two lowest phonons.

The obtained results are in excellent agreement with theoretical prediction by Preis *et al.*[23] on the mutual influence of flux-flow and phonon resonances in Josephson junctions with ionic barriers. Interaction of oscillating electric field with IR and Raman active phonons leads to formation of polaritons, which slow down the group velocity of light to zero
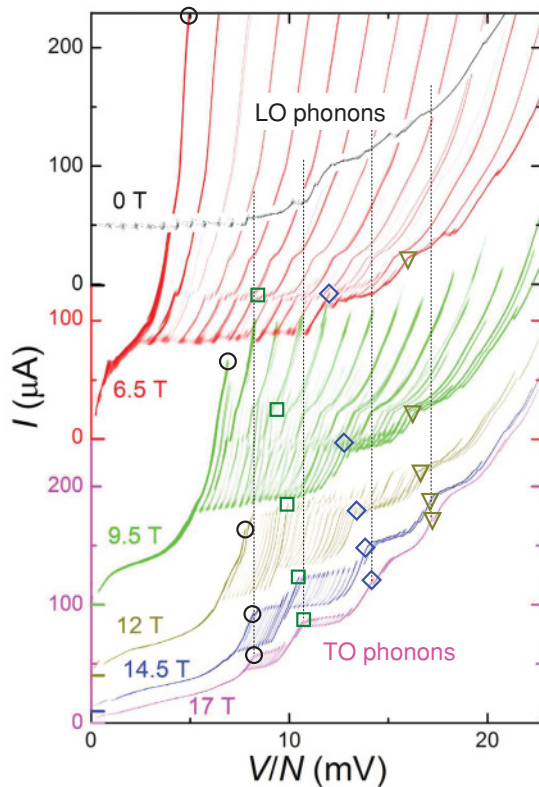

FIG. 3. (Color online) A set of I-V curves for the lead-doped mesa M3 at different in-plane magnetic fields and $T = 1.6$ K. The curves are offset vertically for clarity. Development of the velocity-matching flux-flow resonance (circles) and higher flux-flow and phonon resonances (squares, rhombuses, and triangles) is seen. With increasing H, voltages of flux-flow-phonon resonances first increase and then saturate when the ac Josephson frequency is approaching the next TO phonon frequency (marked by vertical lines). Signs emphasize a gradual transformation of the LO phonon resonance at $H = 0$ to the TO phonon-polariton resonance at $H = 17$ T.
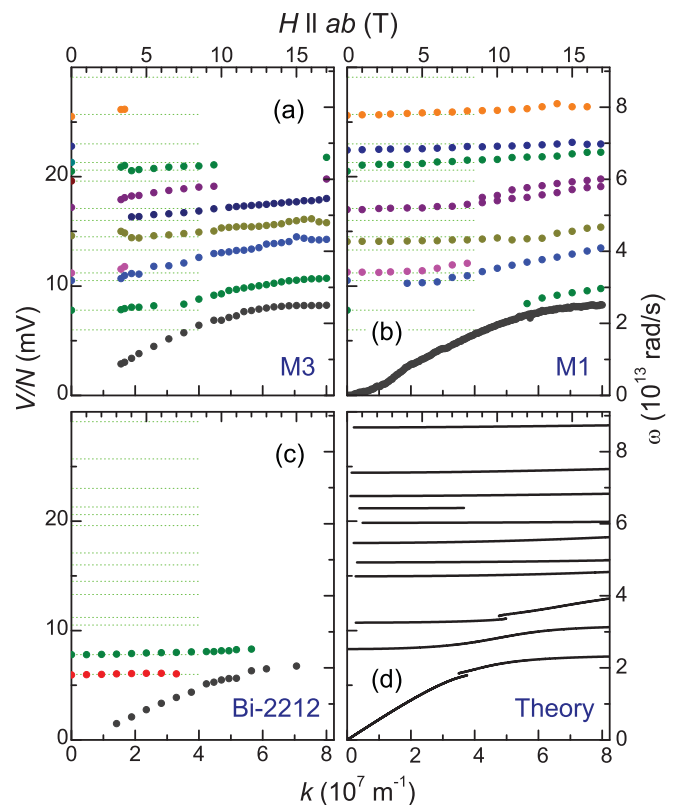

FIG. 4. (Color online) Obtained TEM-wave dispersion relations for (a) mesa M3, (b) mesa M1, and (c) a pure Bi-2212 mesa. Dispersion relations are linear at low frequencies (constant speed of light), but saturate (zero group velocity) whenever the frequency is approaching the TO phonon frequency, indicating formation of polaritons. Panel (d) shows simulated polaritonic dispersion relation from Eq. (1). Horizontal lines represent all observed LO frequencies at $H = 0$.

$d\omega/dk \to 0$ at $\omega \to \omega_{TO}$ and prohibit propagation of TEM waves and flux flow at voltages $\Phi_0\omega_{TO}/2\pi < V_{FF} < \Phi_0\omega_{LO}/2\pi$. This leads to the observed stratification of I-V characteristics in Fig. 3. Our data are well described by the polaritonic dispersion relation of Eq. (1), as shown in Fig. 4(d).

Different selection rules apply for IR and Raman phonons: out-of-phase TEM waves may excite Raman, not IR, and in-phase only IR, not Raman phonons. Due to mutual repulsion, fluxons form a triangular lattice along the regular flux-flow branch and generate out-of-phase TEM waves,[13,21] which excite only Raman, but not IR phonons. This is why the lowest dispersion branch passes the IR phonon number 1 with only a minor kink and forms a polariton with the next Raman phonon number 2, despite the fact that the LO phonon number 1 had a large amplitude at $H = 0$ (see Fig. 1). Similarly, observation of polaritons with IR phonons numbers 3, 5, and 6 at higher dispersion branches demonstrates that the in-phase state, corresponding to the rectangular fluxon lattice, can be stabilized with the help of strong IR phonons. The in-phase state is on demand for achieving coherent high-power THz emission from stacked intrinsic Josephson junctions.[21]

The power, pumped into the phonon-polariton resonance, can be explicitly estimated from the amplitude of steps in I-V's in Fig. 3. It corresponds to kW/cm^2 power density, which can be further enhanced in a coherent[21] or cascade[24] manner using mesas with a larger number of junctions. Thus, Bi-2212 mesas act as a compact and intense source of coherent, monochromatic phonon-polaritons. The phenomenon may be used for creation of a THz phonon laser.[24]

The discovery of phonon-polaritons highlight the unusual electronic structure of cuprates, in which two-dimensional metallic CuO layers are sandwiched between ionic layers. The combination of long-range Coulomb interaction in two-dimensional metallic layers with polar media around them may lead to an unusually strong electron-phonon interaction,[25–28] which may be crucial for high-temperature superconductivity. Presence of the polar response also indicates that it is insufficient to treat cuprates as uniform three-dimensional media, where Coulomb interaction is always well screened. To catch all essential physics of cuprates, theoretical models should take into account their unusual layered metamaterial structure, as revealed in this work.

*vladimir.krasnov@fysik.su.se

[1] Y. Y. Zhu, X. J. Zhang, Y. Q. Lu, Y. F. Chen, Sh. N. Zhu, and N. B. Ming, Phys. Rev. Lett. **90**, 053903 (2003).

[2] J. Brandt, D. Fröhlich, Ch. Sandfort, M. Bayer, H. Stolz, and N. Naka, Phys. Rev. Lett. **99**, 217403 (2007).

[3] Ch. Helm and L. N. Bulaevskii, Phys. Rev. B **66**, 094514 (2002).

[4] V. M. Shalaev, Nat. Photonics **1**, 41 (2007).

[5] A. A. Tsvetkov, D. Dulic, D. van der Marel, A. Damascelli, G. A. Kaljushnaia, J. I. Gorina, N. N. Senturina, N. N. Kolesnikov, Z. F. Ren, J. H. Wang, A. A. Menovsky, and T. T. M. Palstra, Phys. Rev. B **60**, 13196 (1999).

[6] N. N. Kovaleva, A. V. Boris, T. Holden, C. Ulrich, B. Liang, C. T. Lin, B. Keimer, C. Bernhard, J. L. Tallon, D. Munzar, and A. M. Stoneham, Phys. Rev. B **69**, 054511 (2004).

[7] D. N. Basov and T. Timusk, Rev. Mod. Phys. **77**, 721 (2005).

[8] R. Kleiner and P. Müller, Phys. Rev. B **49**, 1327 (1994).

[9] D. Munzar, C. Bernhard, A. Golnik, J. Humlicek, and M. Cardona, Solid State Commun. **112**, 365 (1999).

[10] S. O. Katterwe and V. M. Krasnov, Phys. Rev. B **80**, 020502(R) (2009).

[11] C. J. Wu, M. S. Chen, and T. J. Yang, Phys. C (Amsterdam) **432**, 133 (2005).

[12] S. Savel'ev, V. A. Yampol'skii, A. V. Rakhmanov, and F. Nori, Rep. Prog. Phys. **73**, 026501 (2010).

[13] S. O. Katterwe, A. Rydh, H. Motzkau, A. B. Kulakov, and V. M. Krasnov, Phys. Rev. B **82**, 024517 (2010).

[14] V. M. Krasnov, Phys. Rev. B **79**, 214510 (2009).

[15] K. Schlenga, R. Kleiner, G. Hechtfischer, M. Mößle, S. Schmitt, P. Müller, Ch. Helm, Ch. Preis, F. Forsthofer, J. Keller, H. L. Johnson, M. Veith, and E. Steinbeiß, Phys. Rev. B **57**, 14518 (1998).

[16] Ya. G. Ponomarev, E. B. Tsokur, M. V. Sudakova, S. N. Tchesnokov, M. E. Shabalin, M. A. Lorenz, M. A. Hein, G. Müller, H. Piel, and B. A. Aminov, Solid State Commun. **111**, 513 (1999); E. G. Maksimov, P. I. Arseyev, and N. S. Maslova, *ibid*. **111**, 391 (1999), a different inelastic Cooper-pair tunneling scenario was suggested in this work.

[17] A. Yurgens, Supercond. Sci. Technol. **13**, R85 (2000).

[18] C. Helm, C. Preis, C. Walter, and J. Keller, Phys. Rev. B **62**, 6002 (2000).

[19] M. Kakihana, M. Osada, M. Käll, L. Börjesson, H. Mazaki, H. Yasuoka, M. Yashima, and M. Yoshimura, Phys. Rev. B **53**, 11796 (1996).

[20] V. M. Krasnov, A. E. Kovalev, A. Yurgens, and D. Winkler, Phys. Rev. Lett. **86**, 2657 (2001).

[21] V. M. Krasnov, Phys. Rev. B **82**, 134524 (2010).

[22] There is a small overshooting of the polariton frequency over ω_{LO}. It may be due to non-negligible spatial dispersion of polaritons with zero group velocity; see, e.g., I. Kaelin, Ch. Helm, and G. Blatter, Phys. Rev. B **68**, 012302 (2003). Analysis of this effect requires detailed phonon band structure and lattice dynamics calculations.

[23] C. Preis, C. Helm, K. Schmalzl, J. Keller, R. Kleiner, and P. Müller, Phys. C (Amsterdam) **362**, 51 (2001).

[24] V. M. Krasnov, Phys. Rev. Lett. **97**, 257003 (2006); **103**, 227002 (2009).

[25] C. Falter, Phys. Status Solidi B **242**, 78 (2005).

[26] A. R. Bishop, A. Bussmann-Holder, O. V. Dolgov, A. Furrer, H. Kamimura, H. Keller, R. Khasanov, R. K. Kremer, D. Manske, K. A. Müller, and A. Simon, J. Supercond. Nov. Magn. **20**, 393 (2007).

[27] A. S. Alexandrov and A. M. Bratkovsky, Phys. Rev. Lett. **105**, 226408 (2010).

[28] S. Johnston, F. Vernay, B. Moritz, Z.-X. Shen, N. Nagaosa, J. Zaanen, and T. P. Devereaux, Phys. Rev. B **82**, 064513 (2010).